Research Square

Preprints are preliminary reports that have not undergone peer review.
They should not be considered conclusive, used to inform clinical practice,
or referenced by the media as validated information.

NAT10 Promotes Head and Neck Squamous Cell Carcinoma Progression by Enhancing Autophagy through ac4C-Mediated Suppression of SOCS1

Zhiheng Li
The First Affiliated Hospital of Jinzhou Medical University
Shihang Wang
Shunyi District Hospital
Liang Gong
The First Affiliated Hospital of Jinzhou Medical University
Ming Qian
The First Affiliated Hospital of Jinzhou Medical University
Ruoya Wang
The First Affiliated Hospital of Jinzhou Medical University
Qichuan Jiang
The First Affiliated Hospital of Jinzhou Medical University
Xi Yang
The First Affiliated Hospital of Jinzhou Medical University
Yijie Wang
The First Affiliated Hospital of Jinzhou Medical University
Hao Liu
The First Affiliated Hospital of Jinzhou Medical University
Yin Zhou
The First Affiliated Hospital of Jinzhou Medical University
Zhongyao Liu
The First Affiliated Hospital of Jinzhou Medical University
Mingyu Liu
The First Affiliated Hospital of Jinzhou Medical University
Xuefeng Wang
wangxf@jzmu.edu.cn

First Affiliated Hospital of Jinzhou Medical University

Research Article

Keywords: Head and Neck Squamous Cell Carcinoma (HNSCC), NAT10, N4-acetylcytidine (ac4C), SOCS1, Autophagy, Tumor Progression

Posted Date: October 14th, 2026

DOI: https://doi.org/10.21203/rs.3.rs-10949731/v1

License: This work is licensed under a Creative Commons Attribution 4.0 International License. Read Full License

Additional Declarations: No competing interests reported.

Abstract

Objectives

Head and neck squamous cell carcinoma (HNSCC) has a poor prognosis, highlighting the need to identify new therapeutic targets. N-acetyltransferase 10 (NAT10), the only known enzyme that catalyzes N4-acetylcytidine (ac4C) modification on RNA, has been implicated in tumorigenesis, but its role in HNSCC progression and autophagy remains unclear.

Methods

NAT10 expression and prognostic value in HNSCC were analyzed using TCGA data. Gain- and loss-of-function experiments were performed in HNSCC cells. Cell proliferation, migration, apoptosis, autophagy, and SOCS1 expression were evaluated by functional assays, western blotting, transmission electron microscopy, tandem mRFP-GFP-LC3 assay, RNA immunoprecipitation, and ac4C-RIP followed by qRT-PCR. A subcutaneous xenograft model and immunohistochemistry were used for *in vivo* validation.

Results

Bioinformatics analysis showed that NAT10 was highly expressed in HNSCC tissues and was associated with poor patient prognosis. *In vitro* experiments showed that NAT10 overexpression promoted the proliferation and migration of HNSCC cells and inhibited apoptosis, whereas NAT10 knockdown produced the opposite effects. Mechanistic investigation showed that NAT10 bound to SOCS1 mRNA, and ac4C-RIP further showed that SOCS1 mRNA was enriched in ac4C immunoprecipitates, with significantly increased enrichment after NAT10 overexpression. NAT10 overexpression was associated with reduced SOCS1 expression and increased autophagy in HNSCC cells. Transmission electron microscopy showed increased autophagosome formation after NAT10 overexpression, and the tandem mRFP-GFP-LC3 assay suggested enhanced autophagic flux. Western blot analysis showed that NAT10 overexpression reduced SOCS1 and P62 expression and increased the LC3B-II/LC3B-I ratio and Beclin-1 expression, whereas NAT10 knockdown showed the opposite pattern. In vivo, NAT10 overexpression promoted xenograft tumor growth and was associated with lower SOCS1 expression and higher LC3B expression in tumor tissues.

Conclusions

NAT10 promotes malignant progression of HNSCC and is associated with reduced SOCS1 expression and enhanced autophagy. These findings indicate that NAT10 may serve as a potential therapeutic target in HNSCC.

1. Introduction

Head and neck squamous cell carcinoma (HNSCC) is a common malignancy associated with substantial morbidity and mortality, particularly in patients with recurrent or metastatic disease. Despite multimodal treatment strategies, including surgery, chemotherapy, and radiotherapy, the overall five-year survival rate has not improved markedly in recent years (1, 2). Immunotherapy and molecularly targeted therapies have shown clinical promise in HNSCC (3). However, their overall therapeutic efficacy remains limited, in part because some patients exhibit primary or acquired resistance. A better understanding of the molecular mechanisms underlying HNSCC progression and the identification of novel therapeutic targets therefore remain of considerable clinical importance (1, 4).

N-acetyltransferase 10 (NAT10), a member of the GCN5-related N-acetyltransferase (GNAT) superfamily, is the only known eukaryotic enzyme that catalyzes N4-acetylcytidine (ac4C) modification on RNA (5, 6). ac4C is an important post-transcriptional RNA modification that can influence RNA stability, structure, and translation, thereby affecting gene expression (6, 7). Previous studies have shown that ac4C modification may enhance the stability and translation efficiency of specific target mRNAs, leading to altered protein expression (6, 7).

NAT10 is involved in multiple cellular processes, including ribosome biogenesis, DNA repair, cell cycle regulation, and mRNA translation. Increasing evidence indicates that NAT10 is dysregulated in a variety of human diseases, particularly cancers, in which it is frequently overexpressed and associated with malignant phenotypes such as increased proliferation, migration, invasion, and epithelial-mesenchymal transition (EMT) (6, 8–10). In HNSCC, elevated NAT10 expression has been associated with poor prognosis (11). In addition, recent studies have begun to elucidate its pro-tumorigenic mechanisms, including ac4C-dependent regulation of tRNA, matrix metalloproteinase 1 (MMP1) mRNA, and glycosylated lysosomal membrane protein (GLMP) mRNA (12, 13).

Autophagy is a highly conserved intracellular degradation process that is essential for maintaining cellular homeostasis (14, 15) .In cancer, autophagy exerts context-dependent effects. It may suppress tumor initiation during early stages, whereas in established tumors it often functions as a pro-survival mechanism that promotes adaptation to stress and therapeutic resistance (16, 17). Accordingly, clarification of the molecular mechanisms regulating autophagy may provide a basis for the development of new anti-tumor strategies.

Emerging evidence also suggests that NAT10 may participate in the regulation of autophagy. Under energy stress conditions, sirtuin 1 (Sirt1)-mediated deacetylation of NAT10 has been reported to promote a shift from ribosomal RNA (rRNA) biogenesis to autophagy. More specifically, under nutrient-sufficient conditions, NAT10 binds to and acetylates the K228 site of cell cycle and apoptosis regulator 1 (Che-1), thereby suppressing its transcriptional activity and inhibiting autophagy. Under energy stress conditions, Sirt1-mediated deacetylation of NAT10 relieves this inhibitory effect and promotes autophagy (18). These findings suggest that the acetylation status of NAT10 may be closely related to its role in autophagy regulation.

Suppressor of cytokine signaling 1 (SOCS1) is a well-recognized member of the SOCS family and is widely regarded as a tumor suppressor (19). SOCS1 negatively regulates multiple cytokine signaling pathways and is involved in the control of cell growth, differentiation, apoptosis, and immune responses (20). Reduced expression or functional inactivation of SOCS1 has been reported in multiple tumor types and is often associated with tumor progression and unfavorable clinical outcomes (21). In addition, previous studies have shown that SOCS1 protein can interact with autophagy-related proteins and undergo degradation through the autophagy pathway, thereby influencing tumor cell senescence and apoptosis (22). These findings raise the possibility that autophagy may participate in the regulation of SOCS1 activity.

Although the oncogenic role of NAT10 in HNSCC has been increasingly recognized, and both NAT10 and SOCS1 have been implicated in autophagy-related processes, the precise mechanism by which NAT10 regulates SOCS1 and thereby affects autophagy in HNSCC remains unclear. In particular, it is still unknown whether NAT10 modulates SOCS1 through ac4C-related regulation and whether this process contributes to the malignant progression of HNSCC. Clarifying this mechanism may improve the understanding of HNSCC pathogenesis and may also provide a potential basis for the identification of new therapeutic targets.

The present study was therefore designed to investigate the expression and biological functions of NAT10 in HNSCC and to further explore its role in the regulation of tumor cell autophagy and apoptosis. Particular attention was given to whether NAT10 may regulate SOCS1 through ac4C-related mechanisms, thereby affecting autophagy signaling and promoting malignant progression in HNSCC. By addressing this question, the study sought to provide mechanistic insight into NAT10-mediated HNSCC progression and to evaluate the potential clinical relevance of NAT10 as a therapeutic target.

2. Materials and Methods

2.1. Data Sources and Preprocessing

The Tumor IMmune Estimation Resource (TIMER) database (https://cistrome.shinyapps.io/timer/) was used to compare the expression of NAT10 in different types of cancer. mRNA expression profiles and corresponding clinical data of 546 HNSCC patients were retrieved from the TCGA database (portal.gdc.cancer.gov/projects/TCGA-HNSC). The datasets were combined after normalization. After removing samples with missing clinical data and a follow-up time of 0 days, a final set of 499 HNSCC cases was used for analysis. Survival status and survival time were the clinical factors used. RNA-Seq and clinic data were kept for further analyses. The data analyses were conducted by using R Bioconductor packages.

2.2. Cell Lines and Cell Culture

Cell lines of human HNSCC (Hep2, TU686, FaDu, and Scc-25) and the normal human oral epithelial cell line HOK were obtained from the Cell Bank of the Chinese Academy of Sciences (Shanghai, China). HOK

cells were grown in HOK-specific medium (Sciencell). Hep2, TU686, FaDu, and Scc-25 cells were cultured in RPMI-1640 medium supplemented with 10% fetal bovine serum (FBS) and 1% penicillin-streptomycin, and incubated at 37°C in 5% CO_2 conditions (Thermo Fisher, USA).

2.3. Lentiviral Transduction

TU686 cells were seeded into six-well plates and incubated under standard conditions. Upon reaching 40%–60% confluence, the medium was replaced with Opti-MEM containing polybrene (Thermo Fisher, USA, no. 51985070) for lentiviral transduction (GeneChem, China). The experimental groups included NAT10-overexpressing cells (NAT10 group) and NAT10-knockdown cells (shNAT10 group). Corresponding control groups (NC and shCtrl groups) were transduced with non-targeting lentiviral vectors. After 16–20 h of incubation, the medium was replaced, and after 72 h, cells were selected using puromycin (Merck, Germany, no. 540222) for 48 h. Surviving cells were expanded and stored for subsequent experiments. All lentiviral experiments were conducted in a biosafety level-2 (BSL-2) laboratory in accordance with institutional biosafety guidelines.

2.4. CCK-8 Assay

Cell proliferation was assessed using a Cell Counting Kit-8 (CCK-8) assay (Beyotime, China). TU686 cells from the NAT10, shNAT10, NC, and shCtrl groups were seeded into 96-well plates. Following reagent addition and incubation according to the manufacturer's instructions, absorbance at 450 nm was measured using a microplate reader.

2.5. Wound Healing Assay

Cells from all groups were seeded evenly in 96-well plates and cultured until 80%–90% confluence. Wounds were created using a scratch instrument, and phosphate-buffered saline (PBS) was used to gently remove floating cells. After adding serum-free medium, and images were captured immediately and after 24 hours at the same location. Migration was calculated using the following formula: Wound Healing Rate = (Blank Area at 0 h − Blank Area at 24 h) / Blank Area at 0 h × 100%.

2.6.Transwell Migration Assay

Cell migration was assessed using 24-well Transwell inserts with 8.0-μm pore size membranes (Corning Costar, Corning, NY, USA; cat. no. 3464). TU686 cells from the indicated groups were resuspended in serum-free DMEM, and 5×10^4 cells in 200 μL were seeded into the upper chamber. The lower chamber was filled with 600 μL complete medium containing 10% FBS. After incubation at 37℃ with 5% CO_2 for 24 h, non-migrated cells on the upper surface were removed with a cotton swab. Migrated cells on the lower surface were fixed with 4% paraformaldehyde and stained with 0.1% crystal violet. Images were captured under a light microscope (Olympus, Tokyo, Japan), and migrated cells were counted in five randomly selected fields for statistical analysis.

2.7. Annexin V-FITC/PI Double Staining for Apoptosis Detection

Apoptosis was quantified by flow cytometry using an Annexin V-FITC/PI apoptosis detection kit (Beyotime, China). Cells from each group were harvested, resuspended in sterile PBS, and quantified. About 1 × 10^5 cells were incubated in the dark at room temperature for 20 minutes according to the manufacturer's protocol. Samples were analyzed on ice with a flow cytometer to identify apoptosis levels.

2.8. Western Blot Analysis

TU686 cells from each group were lysed in radioimmunoprecipitation assay (RIPA) buffer. Lysates were cleared by centrifugation at 12,000 rpm for 15 min at 4°C, and protein concentrations were measured using a bicinchoninic acid (BCA) protein assay kit (Beyotime, China, no. P009). Protein samples were prepared and denatured before separation by sodium dodecyl sulfate-polyacrylamide gel electrophoresis (SDS-PAGE) and transfer to polyvinylidene difluoride (PVDF) membranes. Membranes were then blocked with 5% non-fat milk in Tris-buffered saline containing 0.1% Tween-20 (TBST) at room temperature for 1 h, followed by incubation with the primary antibodies overnight at 4°C. The membranes were then incubated with horseradish peroxidase (HRP)-conjugated secondary antibodies for 1 h at room temperature. Signals were developed using an enhanced chemiluminescence (ECL) substrate and detected using a gel imaging system. Band intensities were quantified by densitometric analysis.

The following primary antibodies were used in this study: NAT10 (1:2000, rabbit, Abcam, ab194297), P62 (1:10000, rabbit, Abcam, ab109012), LC3B (1:2000, rabbit, Abcam, ab192890), BCL2 (1:2000, rabbit, Abcam, ab182858), Bax (1:1000, rabbit, Abcam, ab32503), cleaved Caspase-3 and Caspase-3 (1:5000, rabbit, Abcam, ab32351), and SOCS1 (1:1000, rabbit, Abcam, ab280886). The secondary antibody was Goat Anti-Rabbit IgG (1:2000, goat, Abcam, ab150077).

2.9. Transmission Electron Microscopy Observation

TU686 cells in the NAT10 and NC groups were fixed, dehydrated, and embedded for ultrathin sectioning. Sections of approximately 50 nm thickness were prepared using an ultramicrotome and stained with uranyl acetate and lead citrate at room temperature. Autophagosomes were observed under a transmission electron microscope at high magnification. Representative images were captured for subsequent analysis and preserved as raw data.

2.10. ac4C-RNA Immunoprecipitation (ac4C-RIP)–qPCR Assay

To examine whether SOCS1 mRNA carries ac4C modification and whether this modification is affected by NAT10 overexpression, an ac4C-RIP assay was performed using the Magna RIP™ RNA-Binding Protein Immunoprecipitation Kit (Millipore) according to the manufacturer's instructions. Briefly, TU686 cells from the NC and NAT10 overexpression groups were lysed in complete RIP lysis buffer. The cell lysates were then incubated overnight at 4°C with magnetic beads conjugated with an anti-ac4C antibody or normal rabbit IgG as a negative control. After washing, the immunoprecipitated RNA was extracted and purified. The purified RNA was reverse transcribed into complementary DNA (cDNA), and the enrichment

of SOCS1 mRNA in the immunoprecipitates was analyzed by quantitative PCR (qPCR). IgG immunoprecipitation was used as a negative control to assess nonspecific binding. Relative enrichment of SOCS1 mRNA was calculated by comparing the qPCR signal in the ac4C immunoprecipitates with that in the corresponding IgG control. Primer sequences were as follows:

GAPDH-F: GACCTGACCTGCCGTCTA;

GAPDH-R: AGGAGTGGGTGTCGCTGT;

SOCS1-F: GCAGTCTCCACAGCAGCAGAGC;

SOCS1-R: GGAATGTGCGGAAGTGCGTGT.

2.11. Subcutaneous xenograft model

Male BALB/c nude mice (4–5 weeks old, SPF grade) were purchased from Liaoning Changsheng Biotechnology Co., Ltd. (Liaoning, China). All animal experiments were approved by the Ethics Committee of Jinzhou Medical University (Jinzhou, China; approval no. 2024104) and were performed in accordance with institutional guidelines for animal care and use and the principles of the Basel Declaration.

HEp2 cells in the logarithmic growth phase were collected and resuspended in PBS. A total of 5×10^6 cells in 100 μL were subcutaneously injected into the right axillary region of each mouse. For procedures requiring anesthesia, mice were anesthetized by inhalation of isoflurane. Tumor size was measured every 5 days, and tumor volume was calculated using the following formula: volume = (length × width^2)/2. At the end of the experiment, mice were deeply anesthetized with isoflurane and euthanized by cervical dislocation. The tumors were removed and weighed. Tumor tissues were then collected for further histological and immunohistochemical analysis.

2.12. Immunohistochemical analysis

Tumor tissues were collected, fixed in 4% paraformaldehyde, dehydrated through a graded ethanol series, and embedded in paraffin. Paraffin blocks were cut into 4 μm-thick sections for immunohistochemical analysis. After deparaffinization and rehydration, antigen retrieval was performed, followed by blocking of endogenous peroxidase activity and nonspecific binding. The sections were then incubated with primary antibodies against NAT10, SOCS1, and LC3B, followed by incubation with the corresponding secondary antibodies. Immunoreactivity was visualized using DAB, and the sections were counterstained with hematoxylin. Finally, the stained sections were observed and photographed under a light microscope (Olympus, Tokyo, Japan).

2.13. Statistical Analysis

Statistical tests were performed using R Bioconductor packages and GraphPad Prism 7 (or later version). All quantitative data are presented as mean ± standard deviation (SD) from three independent biological replicates (n = 3). Data normality was assessed using the Shapiro-Wilk test. All data

conformed to a normal distribution, justifying the use of parametric tests. For comparing two groups, independent-samples t-tests were used. For comparisons among multiple groups, one-way analysis of variance (ANOVA) followed by Tukey's or Dunnett's post-hoc test was performed. A p-value of less than 0.05 was regarded as statistically significant.

3.Results

3.1. NAT10 is Upregulated in HNSCC and Correlated with Poor Prognosis

To explore the role of NAT10 in HNSCC, the TIMER database was first used to compare NAT10 expression across different tumor types and corresponding normal tissues. The data indicated that NAT10 was significantly elevated in most tumors, including HNSCC (Fig. 1A), suggesting a potential role in tumorigenesis. Analysis of the TCGA-HNSCC dataset further showed that NAT10 mRNA expression was significantly higher in HNSCC tissues than in adjacent normal tissues, with an approximately 1.5-fold increase ($P < 0.01$) (Fig. 1B-D). Survival analysis further showed that higher NAT10 expression was associated with poorer overall survival in patients with HNSCC ($P < 0.01$) (Fig. 1E).

To confirm NAT10 expression at the cellular level in HNSCC, four HNSCC cell lines (Hep2, TU686, FaDu, and SCC-25) and one normal human oral epithelial cell line (HOK) were examined. Western blotting showed that NAT10 protein expression was substantially increased in all four HNSCC cell lines compared with HOK cells (Fig. 1F, 1G). Among them, TU686 cells exhibited the highest NAT10 expression, approximately 3.5-fold higher than that in HOK cells; therefore, TU686 cells were selected for subsequent functional experiments. Taken together, these findings indicate that NAT10 is upregulated in HNSCC tissues and cell lines and is associated with unfavorable clinical outcome.

3.2. NAT10 Modulates HNSCC Cell Proliferation, Migration, and Apoptosis

NAT10 expression was modulated in TU686 cells by lentiviral transduction. Western blot analysis confirmed successful overexpression of NAT10 (NAT10 group) and knockdown of NAT10 (shNAT10 group) compared with the corresponding control groups (NC and shCtrl, respectively). NAT10 overexpression was accompanied by reduced SOCS1 protein expression, whereas NAT10 knockdown increased SOCS1 protein expression (Fig. 2A, 2B).

CCK-8 assays showed that NAT10 overexpression significantly promoted cell proliferation (Fig. 2C, 2D). In addition, wound healing and Transwell migration assays showed that NAT10 overexpression significantly enhanced the migratory ability of TU686 cells (Fig. 2E, 2F). Flow cytometric analysis further showed that NAT10 overexpression significantly reduced the apoptotic rate of TU686 cells (Fig. 2G).

Conversely, NAT10 knockdown significantly inhibited cell proliferation, as shown by CCK-8 assay (Fig. 2H, 2I). Wound healing and Transwell migration assays further showed that NAT10 knockdown

significantly reduced cell migration (Fig. 2J, 2K). In addition, flow cytometric analysis showed that NAT10 knockdown significantly increased apoptosis (Fig. 2L).

3.3. NAT10 Activates Autophagy and Inhibits Apoptosis in HNSCC Cells

To clarify the molecular mechanisms through which NAT10 affects the malignant properties of HNSCC cells, changes in the expression of autophagy-related proteins (P62 and LC3B) and apoptosis-related proteins (Bcl-2, Bax, and Caspase-3) were examined after NAT10 overexpression or knockdown in TU686 cells. Western blot analysis in NAT10-overexpressing TU686 cells showed that P62 expression was significantly decreased, whereas LC3B-II expression was significantly increased. In addition, Bcl-2 expression was increased, whereas Bax and Caspase-3 expression was decreased (Fig. 3A).

Conversely, in NAT10-knockdown TU686 cells, P62 expression was significantly increased, whereas LC3B-II expression was significantly decreased. Meanwhile, Bcl-2 expression was reduced, whereas Bax and Caspase-3 expression was increased (Fig. 3B). These results further support that NAT10 is involved in the regulation of autophagy and apoptosis in HNSCC cells.

To directly visualize the effect of NAT10 on autophagosome formation, transmission electron microscopy (TEM) was used to compare the ultrastructure of NC, NAT10-overexpressing, and shNAT10 TU686 cells. Compared with the NC group, more double-membrane autophagosome-like structures were observed in NAT10-overexpressing cells, whereas fewer such structures were observed in shNAT10 cells (Fig. 3C). These observations support the involvement of NAT10 in the regulation of autophagosome formation.

To further assess autophagic flux, a tandem fluorescent mRFP-GFP-LC3 assay was performed. Compared with the NC group, NAT10-overexpressing cells showed stronger red fluorescence and weaker green fluorescence, suggesting enhanced autophagic flux (Fig. 3D).

3.4. NAT10 suppresses SOCS1 and promotes malignant phenotypes and autophagy in HNSCC cells

To clarify the mechanism underlying the oncogenic effects of NAT10 and the involvement of SOCS1, ac4C-RIP followed by qPCR was performed in NC and NAT10-overexpressing TU686 cells. Western blot analysis first confirmed successful overexpression of NAT10 in TU686 cells (Fig. 4A). qPCR analysis showed that SOCS1 mRNA was barely detectable in the IgG immunoprecipitates in either group, indicating minimal nonspecific binding. By contrast, SOCS1 mRNA was enriched in the ac4C immunoprecipitates, and this enrichment was significantly increased in NAT10-overexpressing cells compared with the NC group (Fig. 4B).

To determine whether the oncogenic activity of NAT10 is mediated through suppression of SOCS1, SOCS1 was co-expressed in NAT10-overexpressing TU686 cells. Successful modulation of NAT10 and SOCS1 was confirmed at both the protein and mRNA levels. Western blot analysis showed that NAT10

protein expression was elevated in the NAT10 group and remained elevated in the NAT10 + SOCS1 group, whereas SOCS1 protein expression, which was reduced by NAT10 overexpression, was restored in the NAT10 + SOCS1 group (Fig. 4C). Consistently, qPCR analysis showed that NAT10 overexpression increased NAT10 mRNA levels (Fig. 4D) and reduced endogenous SOCS1 mRNA levels, and this reduction was reversed by co-expression of exogenous SOCS1 (Fig. 4E).

Functional assays further indicated that re-expression of SOCS1 partially reversed the malignant phenotype induced by NAT10. CCK-8 assays showed that NAT10 overexpression significantly promoted cell growth over 5 days, whereas SOCS1 co-expression partially but significantly attenuated this effect (Fig. 4F, 4G). Similarly, wound healing assays showed that the enhanced migratory capacity induced by NAT10 overexpression was significantly reduced by SOCS1 co-expression (Fig. 4H).

In addition, restoration of SOCS1 reversed the effects of NAT10 on autophagy- and apoptosis-related proteins. Western blot analysis showed that NAT10 overexpression reduced P62 expression and increased LC3B-II and Bcl-2 expression, while decreasing Bax and Caspase-3 expression, suggesting enhanced autophagy and reduced apoptosis. These changes were partially reversed by SOCS1 co-expression, with increased P62 and decreased LC3B-II and Bcl-2 levels, together with increased Bax and Caspase-3 levels (Fig. 4I). Flow cytometric analysis further showed that NAT10 overexpression reduced apoptosis, whereas SOCS1 co-expression significantly weakened this anti-apoptotic effect; SOCS1 overexpression alone markedly increased apoptosis (Fig. 4J).

3.5. Pharmacological modulation of autophagy partially reverses the effects of NAT10 manipulation in HNSCC cells

To further assess whether NAT10 regulates HNSCC cell behavior through the autophagy pathway, the autophagy inhibitor 3-methyladenine (3-MA) and the proteasome inhibitor MG132, which has been widely used to induce autophagy, were used. In NAT10-overexpressing TU686 cells, western blot analysis showed that 3-MA treatment partially reversed the protein changes induced by NAT10 overexpression, as indicated by increased SOCS1 and P62 expression and decreased LC3B expression compared with the NAT10 group (Fig. 5A). CCK-8 assays further showed that NAT10 overexpression promoted cell growth, whereas 3-MA treatment partially attenuated this effect (Fig. 5B, 5C).

In NAT10-silenced TU686 cells, western blot analysis showed that MG132 partially reversed the protein changes induced by NAT10 knockdown, as indicated by decreased SOCS1 and P62 expression and increased LC3B expression in the shNAT10 + MG132 group compared with the shNAT10 group (Fig. 5D). CCK-8 assays further showed that MG132 treatment increased cell growth in both the control and NAT10-overexpressing cells (Fig. 5E, 5F).

3.6. NAT10 promotes HNSCC growth *in vivo*

To assess the role of NAT10 in HNSCC progression *in vivo*, a subcutaneous xenograft model was established. NAT10 overexpression significantly increased tumor growth compared with the NC group, with larger tumor volumes during the observation period and higher tumor weight at the endpoint (Fig. 6A-C). Immunohistochemical staining showed higher NAT10 expression, lower SOCS1 expression, and higher LC3B expression in tumor tissues from the NAT10 overexpression group (Fig. 6D).

4. Discussion

HNSCC remains a significant clinical challenge due to its aggressive nature and limited therapeutic advancements, underscoring the need for novel molecular targets (23, 24). This study investigated the role of NAT10 in HNSCC, providing evidence that NAT10 is overexpressed and promotes pro-tumorigenic phenotypes in HNSCC cells and *in vivo*, in part by modulating autophagy. The findings further suggest that NAT10 may suppress SOCS1 through ac4C-related regulation and thereby contribute to autophagy activation.

Our observation that NAT10 is upregulated in HNSCC and correlates with poor patient prognosis is consistent with its established oncogenic roles across various malignancies (8–11). The enhanced proliferation, migration, and apoptosis resistance conferred by NAT10 overexpression in HNSCC cells align with its known functions in promoting cell cycle progression and EMT in other cancer contexts (6). Recent studies have further highlighted that NAT10 can regulate multiple RNA substrates through ac4C modification and influence diverse biological processes, including metabolism, cell cycle regulation, DNA damage response, autophagy, apoptosis, immune-associated signaling, and oncogenic pathways (25, 26).

While previous studies in related head and neck cancers, such as oral squamous carcinoma (OSCC) and nasopharyngeal carcinoma (NPC), have implicated NAT10-mediated ac4C modification in regulating targets like MMP1 or pathways involving DEAD-box helicase 5 (DDX5) and helicase-like transcription factor (HLTF), which influence tumor growth and metastasis (12, 13), the present findings identify SOCS1 as a distinct downstream candidate in HNSCC. This finding expands the known regulatory network of NAT10 in HNSCC. However, SOCS1 is unlikely to be the only downstream target of NAT10 in HNSCC. NAT10 may regulate additional ac4C-modified transcripts or signaling pathways that also contribute to tumor progression. Unlike targets such as MMP1, which directly promote invasion, or GLMP, which remodels the tumor microenvironment (12), SOCS1 may link RNA modification with autophagy and apoptosis regulation. These pathways may not act independently, but may cooperate in promoting HNSCC progression. Therefore, NAT10-dependent regulation of SOCS1 may represent one important aspect of NAT10 function in head and neck tumorigenesis. At the same time, the current data support SOCS1 as an important downstream effector, but not the sole mediator, of NAT10 function in HNSCC.

A key finding of this study is the capacity of NAT10 to enhance autophagy in HNSCC cells. Autophagy's role in cancer is notably complex, exhibiting dual functions that are context-dependent; it can suppress early tumorigenesis but often supports tumor cell survival and therapeutic resistance in established

tumors (16, 17). In our HNSCC model, NAT10-induced autophagy appears to exert a pro-survival effect, facilitating cellular proliferation and migration while inhibiting apoptosis, thereby contributing to malignant phenotypes. Importantly, in addition to the changes in P62 and LC3B expression and the results of pharmacological intervention, the newly added tandem fluorescent autophagy assay further supported an association between NAT10 modulation and altered autophagic activity, thereby strengthening the conclusion that autophagy is functionally involved in the NAT10-mediated phenotype.

The precise mechanism by which NAT10 modulates autophagy in HNSCC, particularly its interaction with specific targets, has been largely undefined. While Liu et al. demonstrated that Sirt1-mediated deacetylation of NAT10 itself can shift its activity to promote autophagy by relieving inhibition of Che-1 under energy stress (18), our findings suggest an alternative, SOCS1-dependent pathway. NAT10 was found to bind SOCS1 mRNA, and ac4C-RIP analysis provided additional evidence that SOCS1 mRNA was enriched in the ac4C immunoprecipitates, with significantly increased enrichment after NAT10 overexpression. Given NAT10's established function as an ac4C writer, these findings support the possibility that NAT10 may regulate SOCS1 through ac4C-related mechanisms. Such modification could subsequently impair SOCS1 mRNA stability and/or translation efficiency, leading to the observed downregulation of SOCS1 protein. This proposed cascade offers a mechanistic link between NAT10-mediated RNA acetylation and autophagy regulation. However, direct assessment of ac4C levels on SOCS1 mRNA and detailed analysis of its metabolic fate are crucial future steps to substantiate this hypothesis. further work will be required to determine whether NAT10-dependent ac4C modification affects SOCS1 mRNA stability, translation efficiency, or both.

SOCS1 is typically regarded as a tumor suppressor, and its downregulation is frequently associated with increased tumor aggressiveness and poor prognosis (19). Our data suggest that NAT10 may contribute to SOCS1 inactivation in HNSCC, potentially through an ac4C-dependent epigenetic mechanism. Interestingly, Li et al. previously reported that SOCS1/2 proteins can be targeted for degradation via the autophagy pathway (22). This raises the intriguing possibility of a feed-forward loop: NAT10-mediated downregulation of SOCS1 (potentially via ac4C) could initiate autophagy, which, in turn, might further degrade any remaining SOCS1 protein, thereby amplifying NAT10's oncogenic effects. Direct investigation into whether NAT10-induced autophagy contributes to SOCS1 protein degradation is warranted. Moreover, because SOCS1 is a classical negative regulator of JAK/STAT signaling and participates in the feedback control of multiple cytokine-related pathways, the biological consequences of NAT10-mediated SOCS1 suppression may extend beyond autophagy and apoptosis to broader inflammatory or signaling programs. However, these possibilities were not directly examined in the present study and should therefore be interpreted cautiously.

Pharmacological experiments using the autophagy inhibitor 3-MA lend further support to the central role of autophagy in mediating NAT10 effects. Treatment with 3-MA partially rescued SOCS1 expression and reversed the autophagy-related molecular changes in NAT10-overexpressing cells, concurrently attenuating their pro-growth phenotype. These findings collectively underscore autophagy as a significant downstream effector pathway in NAT10-driven HNSCC cell behavior. Similarly, MG132

partially reversed the molecular and phenotypic changes associated with NAT10 manipulation, further supporting the involvement of autophagy in this process. Nevertheless, the partial nature of these rescue effects also suggests that additional NAT10-regulated targets or overlapping signaling pathways may contribute to the observed phenotypes. Therefore, although SOCS1 rescue supports functional involvement of this pathway, it cannot completely exclude parallel or alternative downstream mechanisms.

This work significantly advances our understanding of NAT10 in HNSCC by not only confirming its oncogenic role but also by identifying autophagy induction as a key functional consequence and proposing a detailed molecular mechanism involving SOCS1 regulation, potentially mediated by ac4C. The delineation of this NAT10-SOCS1-autophagy axis offers a novel perspective on HNSCC tumorigenesis. Disrupting this axis, perhaps through emerging NAT10 inhibitors like Remodelin, which have shown preclinical anti-tumor activity, could represent a viable therapeutic strategy for HNSCC, and our findings provide a mechanistic rationale for such approaches. However, the therapeutic feasibility of NAT10 targeting should be interpreted with caution. Because NAT10 has pleiotropic cellular functions and regulates multiple RNA substrates, systemic inhibition may entail on-target or off-target toxicity. Therefore, issues such as target selectivity, therapeutic window, drug delivery, and potential adverse effects require further investigation before clinical translation can be considered.

Nevertheless, this study has several limitations. Although SOCS1 was identified as an important downstream target, NAT10 may also regulate other ac4C-modified mRNAs or pathways in HNSCC. Therefore, the NAT10–SOCS1 pathway described here may represent only part of the broader regulatory network controlled by NAT10. In addition, although our findings support an association between NAT10 and SOCS1 regulation, direct evidence for NAT10-catalyzed ac4C modification of SOCS1 mRNA and its precise effects on mRNA stability or translation efficiency is still needed. In addition, the *in vitro* findings were mainly obtained using established cell lines, which may not fully reflect the heterogeneity of primary HNSCC. Only one normal epithelial cell line was included as a non-malignant control, which also represents a limitation. Furthermore, some public database analyses used in this study were based on computational estimates and heterogeneous clinical datasets, and these factors should be taken into account when interpreting the clinical relevance of the findings. In addition, although Annexin V-FITC/PI staining was used to assess apoptotic changes, this assay does not always allow a strict distinction between late apoptosis and necrosis and does not by itself provide direct mechanistic insight into the upstream events leading to apoptosis. Another important limitation is that HPV status was not evaluated in this study. Because the TU686 cell line used here is HPV-negative, the current conclusions mainly reflect an HPV-negative HNSCC context. Whether NAT10 exerts similar effects, or whether the NAT10/SOCS1/autophagy axis behaves differently, in HPV-positive HNSCC remains unclear and warrants further investigation. In addition, although in vivo xenograft validation has now been included, the models used in this study still do not fully capture the full biological heterogeneity of HNSCC in patients.

Future research should therefore focus on validating the role of NAT10 in HNSCC in vivo and further clarifying the broader NAT10-dependent ac4C regulatory network in this disease. It will also be important to investigate whether NAT10 regulates additional downstream targets or pathways beyond SOCS1. In addition, further studies are needed to determine the precise molecular consequences of NAT10-mediated regulation of SOCS1, including its effects on mRNA stability and translation. Although SOCS1 is known to be involved in cytokine signaling and immune regulation, the possible relationship between NAT10, SOCS1, and immune-related pathways in HNSCC remains unclear and requires further investigation. Further validation in patient-derived materials and more clinically relevant models may also help to better define the translational significance of these findings. Larger clinical cohorts, patient-derived xenografts, organoids, and HPV-positive HNSCC models may be particularly valuable for future validation.

In conclusion, this study identifies NAT10 as a promoter of malignant phenotypes in HNSCC. Our findings suggest that NAT10 may downregulate SOCS1 expression through binding to SOCS1 mRNA and possible ac4C-related regulation, thereby promoting autophagy and contributing to tumor cell proliferation, migration, and apoptosis resistance. These results provide new insight into the role of NAT10 in HNSCC and suggest that NAT10 may serve as a potential therapeutic target in this disease.

Abbreviations

Head and Neck Squamous Cell Carcinoma (HNSCC)

N-acetyltransferase 10 (NAT10)

N4-acetylcytidine (ac4C)

GCN5-related N-acetyltransferase (GNAT)

Ribosomal RNA (rRNA)

Suppressor of Cytokine Signaling 1 (SOCS1)

RNA immunoprecipitation (RIP)

Quantitative PCR (qPCR)

Oral squamous carcinoma (OSCC)

Nasopharyngeal carcinoma (NPC)

Declarations

Acknowledgements

Not applicable

Clinical trial number

Not applicable.

Funding

Contract Number: 2024012017-JH4/4800, Liaoning Province Science and Technology Plan Joint Program (Natural Science Foundation - General Project)

Availability of data and materials

The datasets analyzed during the current study are publicly available. The Tumor IMmune Estimation Resource (TIMER) was used for pan-cancer differential expression analysis of NAT10 (Diff Exp module; https://cistrome.shinyapps.io/timer/; no accession number is assigned to this web-based analysis resource). The TCGA HNSCC cohort is available through the Genomic Data Commons (GDC) Data Portal under project ID TCGA-HNSC (https://portal.gdc.cancer.gov/projects/TCGA-HNSC). Independent validation datasets are available from the Gene Expression Omnibus (GEO) under accession numbers GSE30784 (https://www.ncbi.nlm.nih.gov/geo/query/acc.cgi?acc=GSE30784), GSE23036 (https://www.ncbi.nlm.nih.gov/geo/query/acc.cgi?acc=GSE23036), GSE33205 (https://www.ncbi.nlm.nih.gov/geo/query/acc.cgi?acc=GSE33205), and GSE59102 (https://www.ncbi.nlm.nih.gov/geo/query/acc.cgi?acc=GSE59102). Further original data supporting the findings of this study are available from the corresponding author upon reasonable request.

Authors' contributions

Li Zhiheng: Data management; form analysis; investigation; methodology; writing - original draft; writing - review and editing. Wang Shihang: Data curation; methodology; writing - first draft; writing - review and editing. Gong Liang: Data curation; methodology; writing - first draft; writing - review and editing. Qian Ming: Form analysis; methodology; writing - review and editing. Wang Ruoya: Form analysis; methodology; writing - review and editing. Jiang Qichuan: Form analysis; methodology; writing - review and editing. Yang Xi: Form analysis; methodology; writing - review and editing. Wang Yijie: Form analysis; methodology; writing - review and editing. Liu Hao: Data curation; writing - review and editing. Zhou Yin: Form analysis; methodology; writing - first draft; writing - review and editing. Zhongyao Liu: Form analysis; methodology; writing - first draft; writing - review and editing. Mingyu Liu: Form analysis; methodology; writing - first draft; writing - review and editing.Wang Xuefeng: Project management.

Ethics approval and consent to participate

This study utilized publicly available data from The Cancer Genome Atlas (TCGA) database. As these data are de-identified and publicly accessible, additional institutional review board (IRB) approval was not required for their use. The human cell lines used in this study were obtained from established

commercial cell banks and their use for in vitro research does not require specific ethical approval. All animal experiments were approved by the Ethics Committee of Jinzhou Medical University (Jinzhou, China; approval no. 2024104). All procedures involving animals were conducted in accordance with institutional guidelines for the care and use of laboratory animals and the principles of the Basel Declaration.

Patient consent for publication

Not Applicable.

Competing interests

The authors declare that they have no competing interests.

References

1. Barsouk A, Aluru JS, Rawla P, Saginala K, Barsouk A. Epidemiology, Risk Factors, and Prevention of Head and Neck Squamous Cell Carcinoma. Med Sci (Basel Switzerland). 2023;11:42.
2. Sung H, Ferlay J, Siegel RL, Laversanne M, Soerjomataram I, Jemal A, Bray F. Global Cancer Statistics 2020: GLOBOCAN Estimates of Incidence and Mortality Worldwide for 36 Cancers in 185 Countries. Cancer J Clin. 2021;71:209–49.
3. von Witzleben A, Wang C, Laban S, Savelyeva N, Ottensmeier CH. HNSCC: Tumour Antigens and Their Targeting by Immunotherapy. Cells. 2020;9:2103.
4. Guo Z, Li K, Ren X, Wang X, Yang D, Ma S, Zeng X, Zhang P. The role of the tumor microenvironment in HNSCC resistance and targeted therapy. Front Immunol. 2025;16:1554835.
5. Dominissini D, Rechavi G. N(4)-acetylation of Cytidine in mRNA by NAT10 Regulates Stability and Translation. Cell. 2018;175:1725–7.
6. Xie L, Zhong X, Cao W, Liu J, Zu X, Chen L. Mechanisms of NAT10 as ac4C writer in diseases. Molecular therapy. Nucleic acids. 2023;32:359–68.
7. Xiang Y, Zhou C, Zeng Y, Guo Q, Huang J, Wu T, Liu J, Liang Q, Zeng H, Liang X. NAT10-Mediated N4-Acetylcytidine of RNA Contributes to Post-transcriptional Regulation of Mouse Oocyte Maturation in vitro. Front Cell Dev Biol. 2021;9:704341.
8. Yang C, Wu T, Zhang J, Liu J, Zhao K, Sun W, Zhou X, Kong X, Shi J. Prognostic and Immunological Role of mRNA ac4C Regulator NAT10 in Pan-Cancer: New Territory?for. Cancer Research? Front Oncol. 2021;11:630417.
9. Pan Z, Bao Y, Hu M, Zhu Y, Tan C, Fan L, Yu H, Wang A, Cui J, Sun G. Role of NAT10-mediated ac4C-modified HSP90AA1 RNA acetylation in ER stress-mediated metastasis and lenvatinib resistance in hepatocellular carcinoma. Cell Death Discov. 2023;9:56.
10. Miao D, Shi J, Lv Q, Tan D, Zhao C, Xiong Z, Zhang X. NAT10-mediated ac(4)C-modified ANKZF1 promotes tumor progression and lymphangiogenesis in clear-cell renal cell carcinoma by

attenuating YWHAE-driven cytoplasmic retention of YAP1. Cancer Commun (London England). 2024;44:361–83.

11. Tao W, Tian G, Xu S, Li J, Zhang Z, Li J. NAT10 as a potential prognostic biomarker and therapeutic target for HNSCC. Cancer Cell Int. 2021;21:413.
12. Liu Y, Wang X, Liu Y, Yang J, Mao W, Feng C, Wu X, Chen X, Chen L, Dong P. N4-acetylcytidine-dependent GLMP mRNA stabilization by NAT10 promotes head and neck squamous cell carcinoma metastasis and remodels tumor microenvironment through MAPK/ERK signaling pathway. Cell Death Dis. 2023;14:712.
13. Xie H, Zhang K, Yin H, Zhang S, Pan S, Wu R, Han Y, Xu Y, Jiang W, You B. Acetyltransferase NAT10 inhibits T-cell immunity and promotes nasopharyngeal carcinoma progression through DDX5/HMGB1 axis. J Immunother Cancer. 2025;13:e10301.
14. Kim J, Yu YS, Choi Y, Lee DH, Han S, Kwon J, Noda T, Ikawa M, Kim D, Kim H, et al. USF2 and TFEB compete in regulating lysosomal and autophagy genes. Nat Commun. 2024;15:8334.
15. Kausar MA, Anwar S, Khan YS, Saleh AA, Ahmed MAA, Kaur S, Iqbal N. Siddiqui WA and Najm MZ: Autophagy and Cancer: Insights into Molecular Mechanisms and Therapeutic Approaches for Chronic Myeloid Leukemia. Biomolecules. 2025;15:215.
16. Jiang T, Chen X, Ren X, Yang J, Cheng Y. Emerging role of autophagy in anti-tumor immunity: Implications for the modulation of immunotherapy resistance. Drug Resist updates: reviews commentaries Antimicrob anticancer Chemother. 2021;56:100752.
17. Debnath J, Gammoh N, Ryan KM. Autophagy and autophagy-related pathways in cancer. Nat Rev Mol Cell Biol. 2023;24:560–75.
18. Liu X, Cai S, Zhang C, Liu Z, Luo J, Xing B, Du X. Deacetylation of NAT10 by Sirt1 promotes the transition from rRNA biogenesis to autophagy upon energy stress. Nucleic Acids Res. 2018;46:9601–16.
19. Beaurivage C, Champagne A, Tobelaim WS, Pomerleau V, Menendez A, Saucier C. SOCS1 in cancer: An oncogene and a tumor suppressor. Cytokine. 2016;82:87–94.
20. Bidgood GM, Keating N, Doggett K, Nicholson SE. SOCS1 is a critical checkpoint in immune homeostasis, inflammation and tumor immunity. Front Immunol. 2024;15:1419951.
21. Gu C, Chen X, Wu J, Zhang Y, Zhong L, Luo H, Luo W, Yang F. SOCS1: A potential diagnostic and prognostic marker for aggressive gliomas and a new target for immunotherapy. Med (Baltim). 2024;103:e40632.
22. Li L, Chen X, Lv M, Cheng Z, Liu F, Wang Y, Zhou A, Liu J, Zhao X. Effect of Platycodon grandiflorus Polysaccharide on M1 Polarization Induced by Autophagy Degradation of SOCS1/2 Proteins in 3D4/21 Cells. Front Immunol. 2022;13:934084.
23. Johnson DE, Burtness B, Leemans CR, Lui VWY, Bauman JE, Grandis JR. Head and neck squamous cell carcinoma. Nat reviews Disease primers. 2020;6:92.
24. Kitamura N, Sento S, Yoshizawa Y, Sasabe E, Kudo Y, Yamamoto T. Current Trends and Future Prospects of Molecular Targeted Therapy in Head and Neck Squamous Cell Carcinoma. Int J Mol

Sci. 2020;22:240.

25. Qin D, Liu Q, Ma X, Wang R, Lu T, Yang Y, Tang Z, Zhu Y. Research progress on NAT10-mediated acetylation in normal development and disease. Front Cell Dev Biol. 2025;13:1623276.

26. Xiao B, Wu S, Tian Y, Huang W, Chen G, Luo D, Cai Y, Chen M, Zhang Y, Liu C, et al. Advances of NAT10 in diseases: insights from dual properties as protein and RNA acetyltransferase. Cell Biol Toxicol. 2024;41:17.

Figures

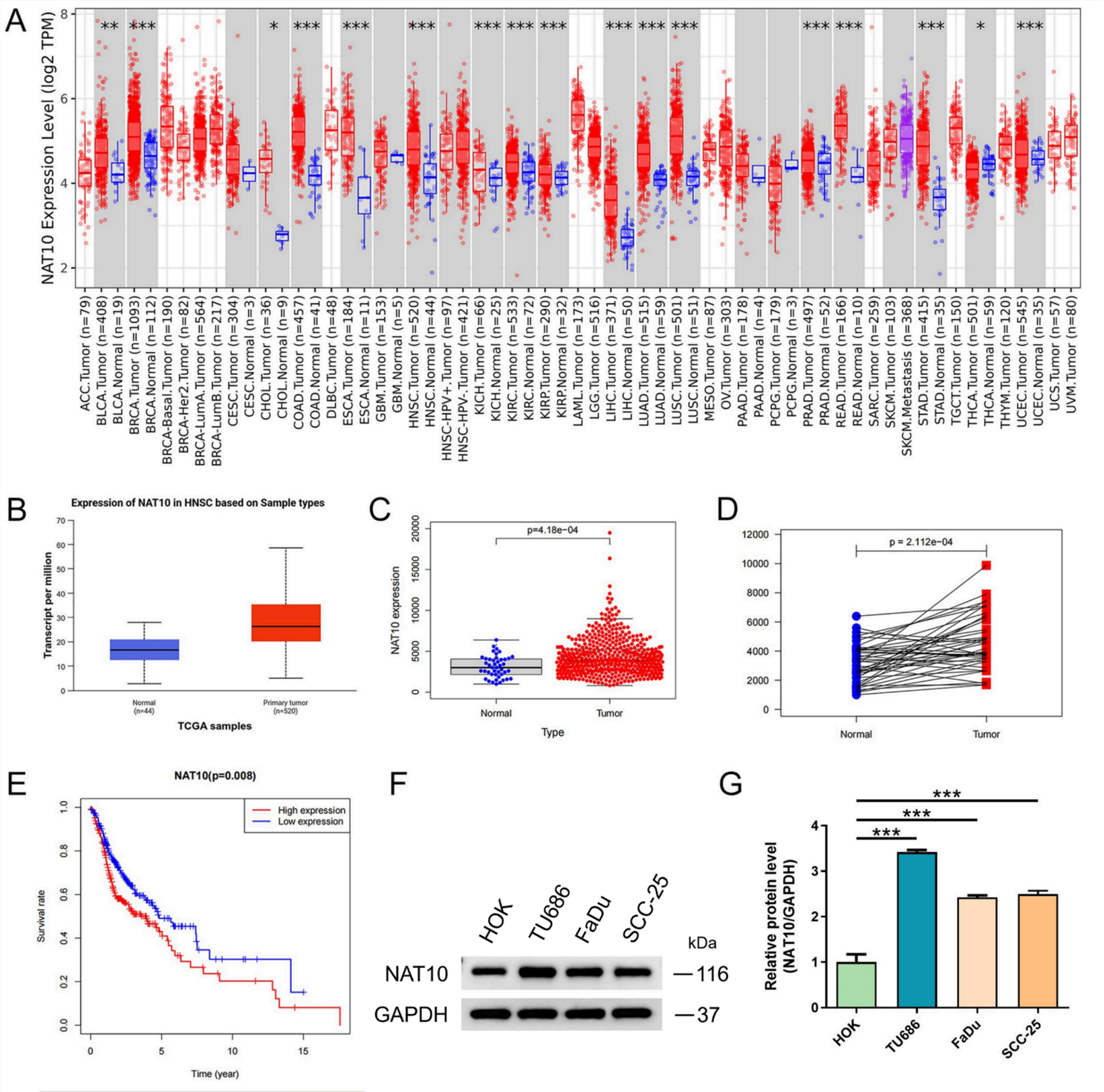


Figure 1

Expression of NAT10 in Head and Neck Squamous Cell Carcinoma (HNSCC).

(A) TIMER database analysis of NAT10 expression patterns across various tumor types.

(B) NAT10 expression in normal tissues and HNSCC tissues based on TCGA data.

(C) Scatter plot showing differential NAT10 expression between normal and HNSCC tissues.

(D) NAT10 mRNA expression in paired normal and HNSCC tissues from TCGA dataset.

(E) Survival analysis showing that high NAT10 expression is associated with poor overall survival in HNSCC patients (grouped according to the median NAT10 expression level; P = 0.008).

(F, G) Western blot analysis showing elevated NAT10 protein expression in HNSCC cell lines compared with HOK cells. TU686 cells were selected for subsequent experiments. Data are presented as mean ±SD from three independent experiments (n=3). ***P < 0.001.

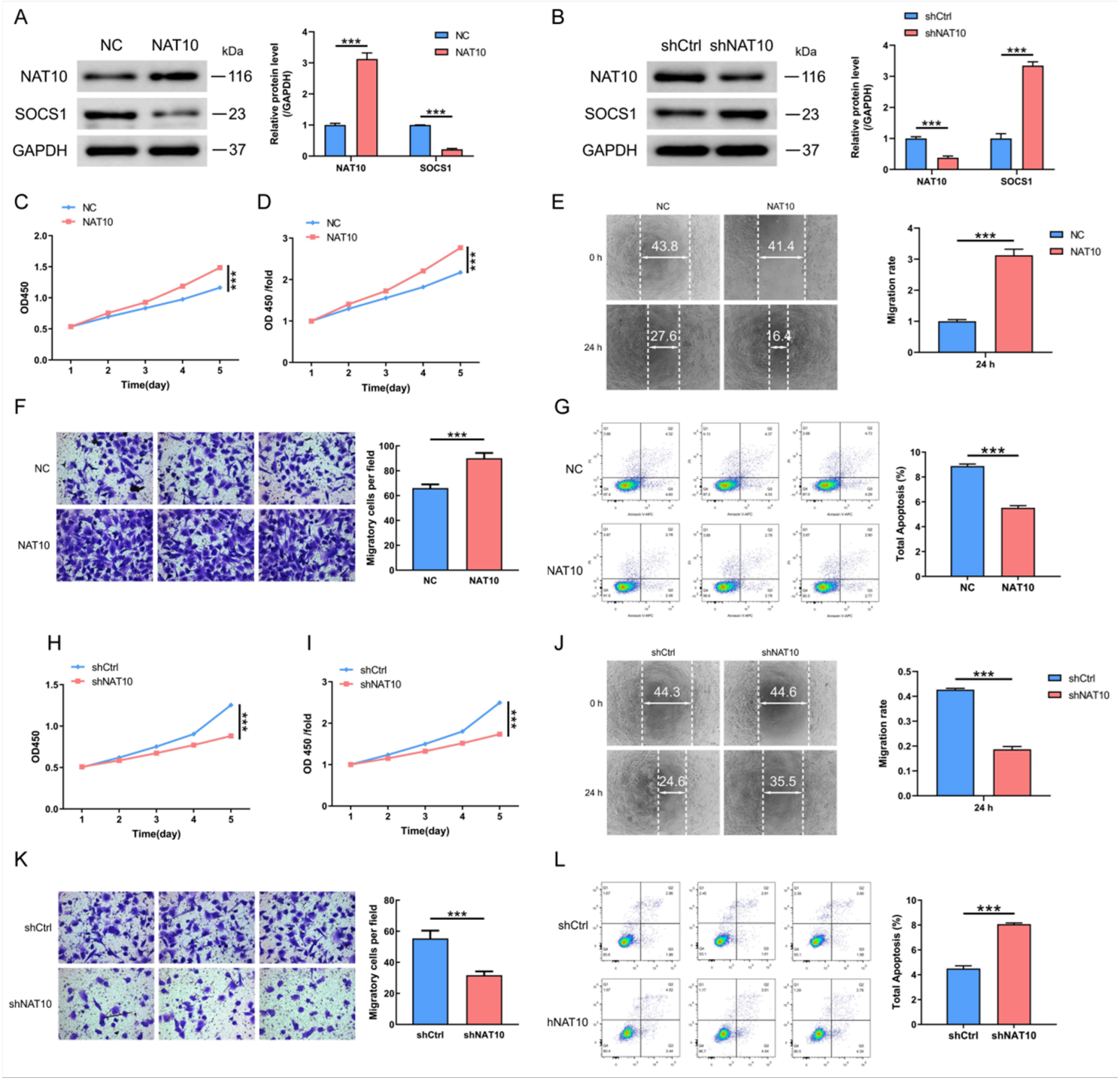


Figure 2

NAT10 modulates proliferation, migration, and apoptosis in HNSCC cells

(A) Western blot and quantitative analysis showing NAT10 and SOCS1 protein expression in NC and NAT10-overexpressing TU686 cells.

(B) Western blot and quantitative analysis showing NAT10 and SOCS1 protein expression in shCtrl and shNAT10 TU686 cells.

(C, D) CCK-8 assay detecting cell proliferation in NC and NAT10-overexpressing TU686 cells.

(E) Wound healing assay and quantitative analysis detecting the migratory ability of NC and NAT10-overexpressing TU686 cells at 24 h.

(F) Transwell migration assay and quantitative analysis detecting the migratory ability of NC and NAT10-overexpressing TU686 cells.

(G) Flow cytometry and quantitative analysis detecting the apoptosis rate of NC and NAT10-overexpressing TU686 cells.

(H, I) CCK-8 assay detecting cell proliferation in shCtrl and shNAT10 TU686 cells.

(J) Wound healing assay and quantitative analysis detecting the migratory ability of shCtrl and shNAT10 TU686 cells at 24 h.

(K) Transwell migration assay and quantitative analysis detecting the migratory ability of shCtrl and shNAT10 TU686 cells.

(L) Flow cytometry and quantitative analysis detecting the apoptosis rate of shCtrl and shNAT10 TU686 cells.

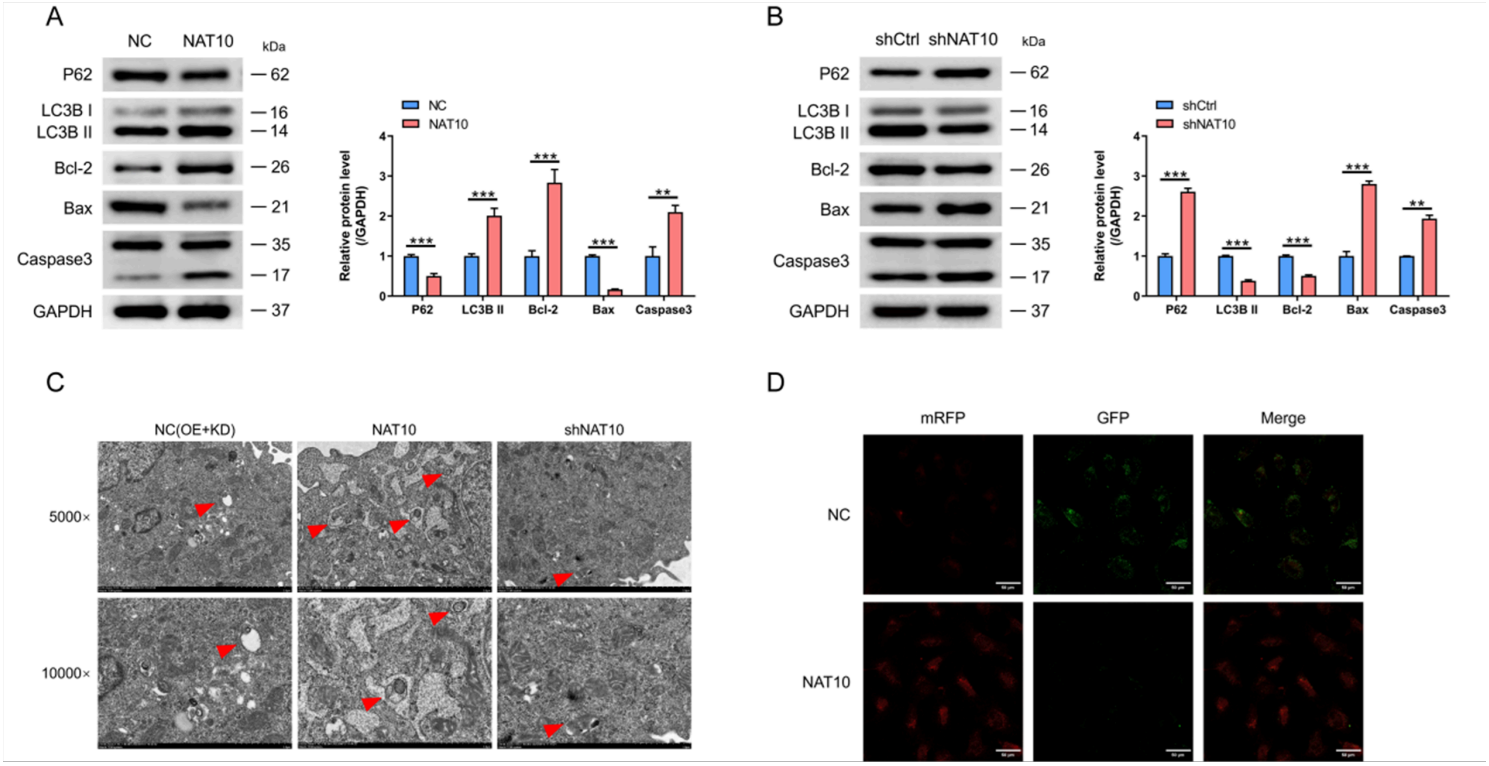


Figure 3

NAT10 activates autophagy and inhibits apoptosis in HNSCC cells

(A) Western blot and quantitative analysis detecting the expression of autophagy- and apoptosis-related proteins (P62, LC3B, Bcl-2, Bax, and Caspase-3) in NC and NAT10-overexpressing TU686 cells.

(B) Western blot and quantitative analysis detecting the expression of autophagy- and apoptosis-related proteins (P62, LC3B, Bcl-2, Bax, and Caspase-3) in shCtrl and shNAT10 TU686 cells.

(C) Transmission electron microscopy images showing ultrastructural changes in NC, NAT10-overexpressing, and shNAT10 TU686 cells. Red arrowheads indicate autophagosome-like structures.

(D) Tandem mRFP-GFP-LC3 fluorescence assay in NC and NAT10-overexpressing TU686 cells. Representative images showing mRFP, GFP, and merged signals. Scale bar = 50 μm.

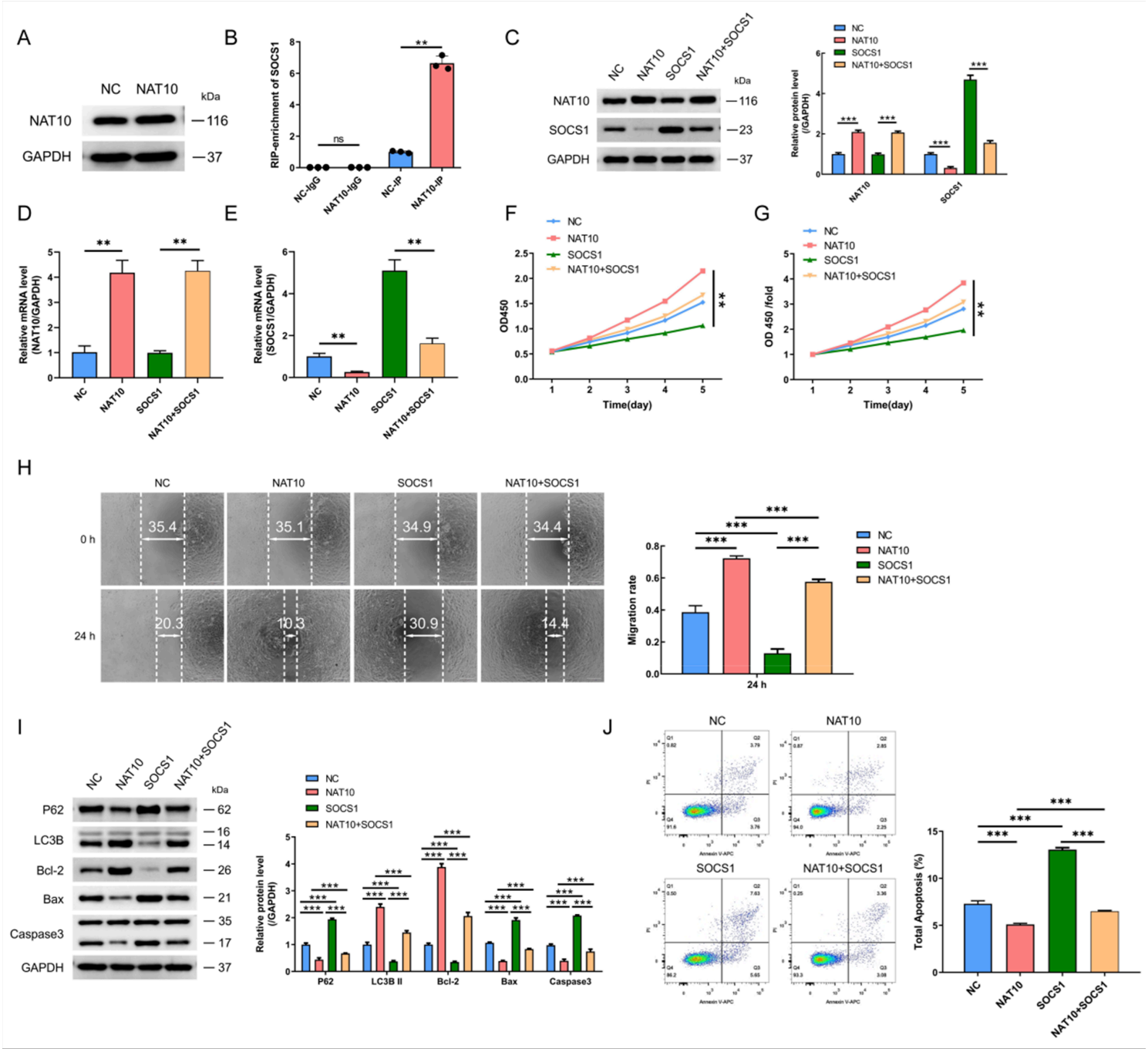


Figure 4

NAT10 promotes ac4C enrichment on SOCS1 mRNA and suppresses SOCS1 to regulate HNSCC malignant phenotypes and autophagy

(A) Western blot detecting NAT10 expression in NC and NAT10-overexpressing TU686 cells.

(B) ac4C-RIP followed by qPCR detecting ac4C enrichment of SOCS1 mRNA in NC and NAT10-overexpressing TU686 cells.

(C) Western blot and quantitative analysis detecting NAT10 and SOCS1 protein expression after NAT10 and SOCS1 overexpression.

(D, E) qRT-PCR detecting NAT10 and SOCS1 mRNA levels after NAT10 and SOCS1 overexpression.

(F, G) CCK-8 assays detecting cell viability in NAT10- and SOCS1-overexpressing cells.

(H) Wound healing assay and quantitative analysis detecting the migratory ability of the indicated groups at 24 h.

(I) Western blot and quantitative analysis detecting the expression of autophagy- and apoptosis-related proteins (P62, LC3B, Bcl-2, Bax, and Caspase-3) after NAT10 and SOCS1 overexpression.

(J) Flow cytometry and quantitative analysis detecting the apoptosis rate of the indicated groups.

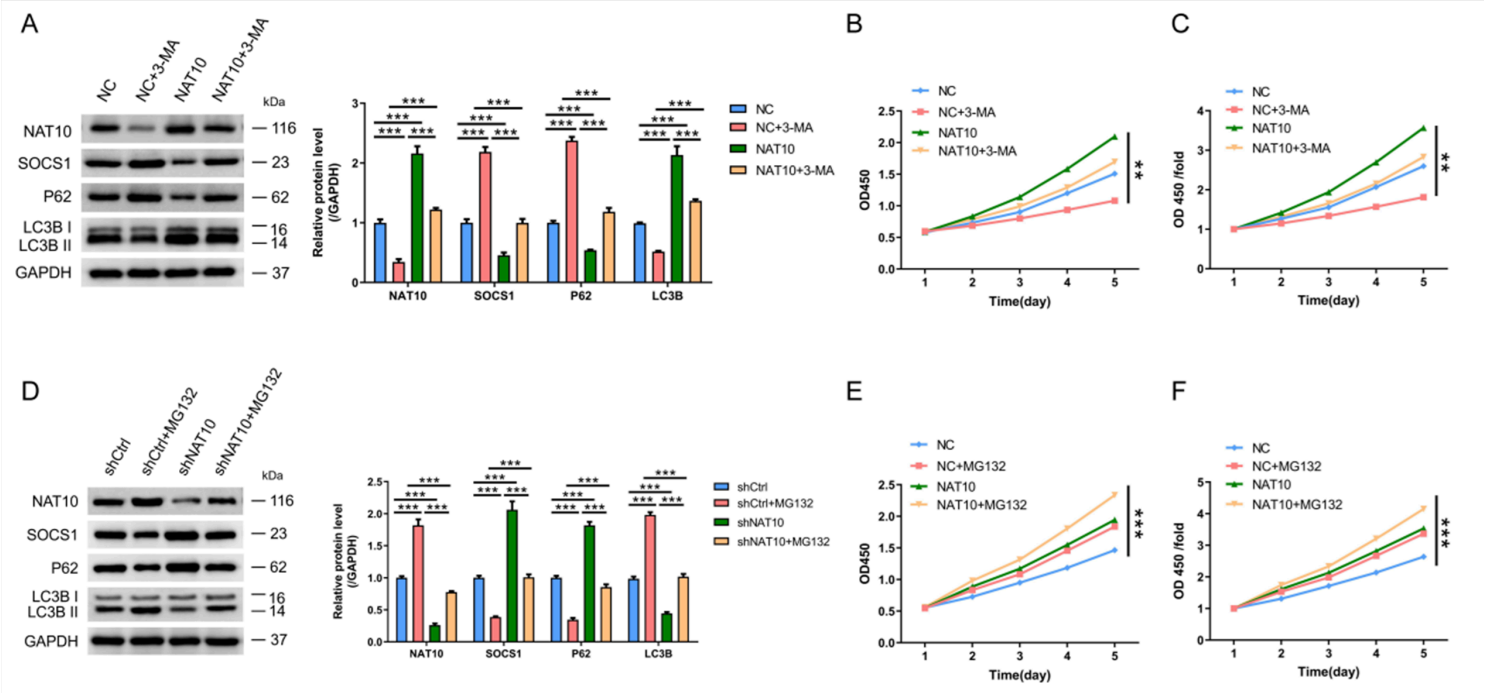


Figure 5

Pharmacological modulation of autophagy partially reverses the effects of NAT10 manipulation in HNSCC cells

(A) Western blot and quantitative analysis detecting NAT10, SOCS1, P62, and LC3B expression in NC, NC+3-MA, NAT10, and NAT10+3-MA TU686 cells.

(B, C) CCK-8 assays detecting cell viability in NC, NC+3-MA, NAT10, and NAT10+3-MA TU686 cells.

(D) Western blot and quantitative analysis detecting NAT10, SOCS1, P62, and LC3B expression in shCtrl, shCtrl+MG132, shNAT10, and shNAT10+MG132 TU686 cells.

(E, F) CCK-8 assays detecting cell viability in NC, NC+MG132, NAT10, and NAT10+MG132 TU686 cells.

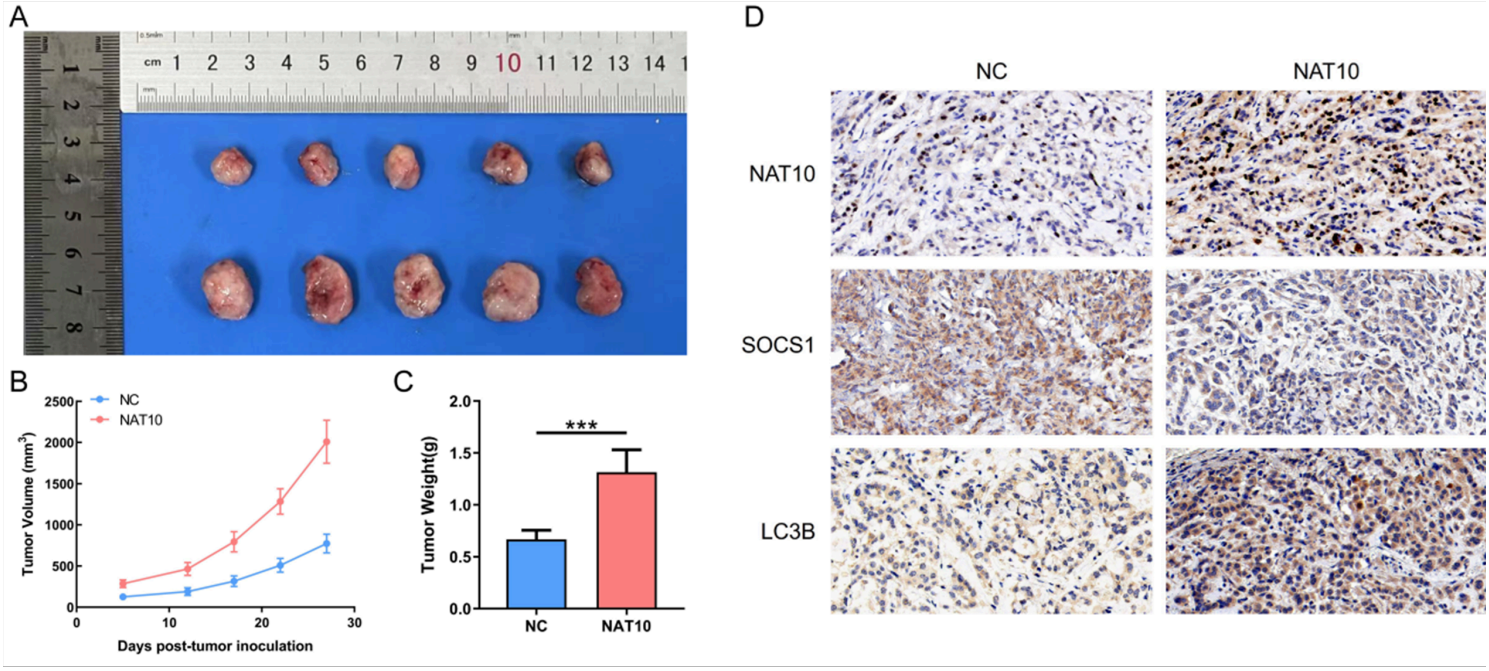


Figure 6

NAT10 overexpression promotes tumor growth *in vivo*.

(A) Representative images of xenograft tumors in the NC and NAT10 overexpression groups;

(B) Tumor growth curves in nude mice;

(C) Tumor weights at the endpoint;

(D) Immunohistochemical staining of NAT10, SOCS1, and LC3B in tumor tissues.

Supplementary Files

This is a list of supplementary files associated with this preprint. Click to download.

- Supplementarymaterial.docx